AD

USAAMRDL TECHNICAL REPORT 71-51

INDUCTIVE SENSING TECHNIQUE ADVANCEMENT

By

George G. Moross

September 1971

EUSTIS DIRECTORATE
U. S. ARMY AIR MOBILITY RESEARCH AND DEVELOPMENT LABORATORY
FORT EUSTIS, VIRGINIA

CONTRACT DAAJ02-70-C-0028
MECHANICAL TECHNOLOGY INCORPORATED
LATHAM, NEW YORK

DISCLAIMERS

The findings in this report are not to be construed as an official Department of the Army position unless so designated by other authorized documents.

When Government drawings, specifications, or other data are used for any purpose other than in connection with a definitely related Government procurement operation, the United States Government thereby incurs no responsibility nor any obligation whatsoever; and the fact that the Government may have formulated, furnished, or in any way supplied the said drawings, specifications, or other data is not to be regarded by implication or otherwise as in any manner licensing the holder or any other person or corporation, or conveying any rights or permission, to manufacture, use, or sell any patented invention that may in any way be related thereto.

Trade names cited in this report do not constitute an official endorsement or approval of the use of such commercial hardware or software.

DISPOSITION INSTRUCTIONS

Destroy this report when no longer needed. Do not return it to the originator.

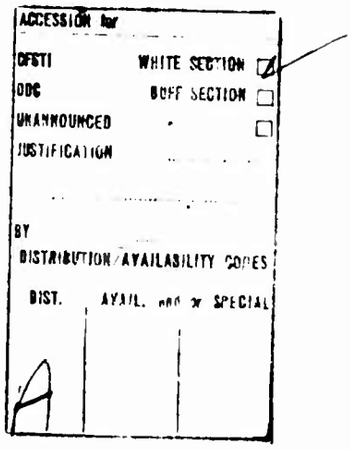

UNCLASSIFIED

Security Classification

DOCUMENT CONTROL DATA - R & D

(Security classification of title, body of abstract and indexing annotation must be entered when the overall report is classified)

1. ORIGINATING ACTIVITY (Corporate author)	2a. REPORT SECURITY CLASSIFICATION
Mechanical Technology Incorporated Latham, New York	Unclassified
	2b. GROUP

3. REPORT TITLE

INDUCTIVE SENSING TECHNIQUE ADVANCEMENT

4. DESCRIPTIVE NOTES (Type of report and inclusive dates)

Final Report

5. AUTHOR(S) (First name, middle initial, last name)

George G. Moross

6. REPORT DATE	7a. TOTAL NO. OF PAGES	7b. NO. OF REFS
September 1971	41	1

8a. CONTRACT OR GRANT NO.	9a. ORIGINATOR'S REPORT NUMBER(S)
DAAJ02-70-C-0028	
b. PROJECT NO.	USAAMRDL Technical Report 71-51
Task 1F162203A43405	
c.	9b. OTHER REPORT NO(S) (Any other numbers that may be assigned this report)
d.	MTI 71TR41

10. DISTRIBUTION STATEMENT

Approved for public release; distribution unlimited.

11. SUPPLEMENTARY NOTES	12. SPONSORING MILITARY ACTIVITY
	Eustis Directorate, U. S. Army Air Mobility Research and Development Laboratory, Fort Eustis, Virginia

13. ABSTRACT

This program is concerned with the advancement and development of the inductive sensing system first reported in USAAVLABS Technical Report 69-97. The system has been significantly enhanced in its ability to detect early fatigue damage in 6061 T-6 aluminum. Samples have been fatigue cycled up to 2 x 10^6 cycles, and crack signals have been observed as early as 9.7% of life. The system has been greatly enhanced in its sensitivity to cracks and its insensitivity to extraneous factors such as probe proximity and generalized surface damage. This increased sensitivity to flaws, coupled with the ability to selectively disregard extraneous surface conditions or probe proximity, has significantly advanced the state of the art in nondestructive testing.

DD FORM 1 NOV 68 1473 REPLACES DD FORM 1473, 1 JAN 64, WHICH IS OBSOLETE FOR ARMY USE.

UNCLASSIFIED

Security Classification

14. KEY WORDS	LINK A		LINK B		LINK C	
	ROLE	WT	ROLE	WT	ROLE	WT
Metal Fatigue Detection Inductive Detection System Inductive Sensing Fatigue Damage						

DEPARTMENT OF THE ARMY
U S. ARMY AIR MOBILITY RESEARCH & DEVELOPMENT LABORATORY
EUSTIS DIRECTORATE
FORT EUSTIS, VIRGINIA 23604

This report was prepared by Mechanical Technology, Inc., under the terms of Contract DAAJ02-70-C-0028. The objective of this contractual effort was to study, redesign, and evaluate the inductive detection system investigated earlier under a USAAMRDL contract in order to improve its capability to detect early fatigue cracks and to exhibit less sensitivity to extraneous factors.

The work performed under this contract is considered to be quite productive in that, through the application of the rotating probe concept, a high degree of insensitivity to surface and geometric factors was achieved while retaining the stationary probe crack sensitivity. The concept used in this effort appears to have high potential for Army applications.

The conclusions and recommendations contained herein are concurred in by this Directorate.

The technical monitor for this contract was Mr. S. Blair Poteate, Jr.

Task 1F162203A43405
Contract DAAJ02-70-C-0028
USAAMRDL Technical Report 71-51
September 1971

INDUCTIVE SENSING TECHNIQUE ADVANCEMENT

MTI 71TR41

By

George G. Moross

Prepared by

Mechanical Technology Incorporated
Latham, New York

for

EUSTIS DIRECTORATE
U.S. ARMY AIR MOBILITY RESEARCH & DEVELOPMENT LABORATORY
FORT EUSTIS, VIRGINIA

ABSTRACT

This program is concerned with the advancement and development of the inductive sensing system first reported in USAAVLABS Technical Report 69-97. The system has been significantly enhanced in its ability to detect early fatigue damage in 6061 T-6 aluminum. Samples have been fatigue cycled up to 2 x 10^6 cycles, and crack signals have been observed as early as 9.7% of life. The system has been greatly enhanced in its sensitivity to cracks and its insensitivity to extraneous factors such as probe proximity and generalized surface damage. This increased sensitivity to flaws, coupled with the ability to selectively disregard extraneous surface conditions or probe proximity, has significantly advanced the state of the art in nondestructive testing.

FOREWORD

Grateful acknowledgement is made to Mr. Leo Hoogenboom of the MTI staff who was responsible for the development of the rotating probe and Mr. Curt Kissinger who was instrumental in the design.

BLANK PAGE

TABLE OF CONTENTS

LIST OF ILLUSTRATIONS

INTRODUCTION

The objective of this program was to study, redesign and evaluate the inductive detection system first used on Contract DAAJ02-68-C-0005 (see USAAVLABS Technical Report 69-97*), in order to improve its capability to detect early fatigue damage and to exhibit less sensitivity to extraneous factors. The inductive system was originally designed to measure the proximity of a metallic surface to the probe. As a result of preliminary experimentation by the MTI staff, it was noted that a flawed surface produced significant irregularities in the proximity signal. These irregularities were carefully studied in the program and shown to be crack signals. In addition, a series of fatigue samples were run with periodic scanning using the inductive system. These samples were also replicated, sectioned, and examined utilizing metallographic techniques to prove the surface flaws responsible for the signals. During the performance of the above contract, three materials were selected for vibratory beam testing (6061 T-6 aluminum, 9310 steel, and Inconel). The detection system generally showed an equal ability to detect incipient fatigue damage (microcracking) at an early point in the life of the specimen among the three materials selected. Aluminum (6061 T-6) showed the earliest signals and, hence, was selected as the material with which the detection system would be optimized. This material is most widely used in airframes of Army helicopters, and a substantial effort in nondestructive test techniques is required at field service facilities in order to determine the airworthiness of a ship. Inductive detection system is seen as a method by which fatigue cracking can be detected at an incipient stage and thus form a rationale by which a scrap-or-use decision can be made.

---

* INVESTIGATION TO DETERMINE THE FEASIBILITY OF DETECTING IMPENDING METAL FATIGUE FAILURE THROUGH USE OF AN INDUCTIVE SENSING DEVICE, U.S. Army Air Mobility Research and Development Laboratory, Fort Eustis, Virginia, February, 1971, AD 871155.

DISCUSSION

GENERAL COMMENTS

The present contract effort has encompassed the system's future capability for use in a field rather than a laboratory environment. The effect of such surface conditions as paint, anodizing, surface scratching, surface peening, grease, oil and rough machine finish has been seen to have little or no effect on the system's ability to detect microcracks; and in fact, the anodizing allowed a slightly earlier detection of the beginning of fatigue damage. This phenomenon is explained on page 24 of this report. In summary, the system is not affected deleteriously by surface condition as long as the probe can be placed in reasonable proximity to the material to be examined, and the intervening layers (if any) are non-ferromagnetic. In the case of a ferromagnetic material between the probe and the non-ferromagnetic specimen, the flux field from the probe is effectively "shorted out" in that the flux does not penetrate through the material but provides a measurable signal due to inhomogeneities (flaws) in the ferromagnetic material. For example, a non-ferromagnetic material (titanium) .020 inch thick was placed between the probe and aluminum sample #1. This interspersion caused no decrease in the crack signal from the sample (with the proximity compensating circuit connected); however, the same thickness of steel placed between the probe and the sample reduced the crack signal to essentially background level due to the flux being "shorted" by the steel, thus not allowing the field to penetrate into the aluminum.

THEORY OF OPERATION

The inductive sensing system used in the performance of this work consists of a probe, oscillator, bridge circuit, detector, various filters, compensation circuitry developed during this program, and readout devices. The basic probe consists of a "u" shaped core with a winding of copper wire at the center. This coil-core combination is placed in one leg of an AC bridge which is driven by an oscillator. The signal from the bridge is fed to a synchronous detector whose output is a DC voltage corresponding to bridge balance. The probe is positioned such that the sample forms the flux path between the legs of the "u", and the flux passes through the sample material. When the bridge is initially balanced with the probe over good material and then the probe moved to cracked or otherwise flawed material, the bridge will indicate an unbalance due to the change in material properties (cracks, flaws or other inhomogeneities) as long as other factors such as proximity are maintained constant. Since the probe is a reluctance measuring device, any factor which will affect the reluctance of the flux path will cause a change in the bridge balance. For this reason, proximity of the probe to the surface to be examined must be either maintained constant or compensated out electronically.

A major thrust in this program was to design a probe which would increase crack sensitivity, or at least maintain previous sensitivity, and minimize effects due to extraneous factors such as proximity, surface degradation

and surface coatings. The development sequence is discussed on page 9; however, advantage was taken of the fact that an elementary horseshoe probe is highly directional and can generate a proximity compensating signal as well as a sensitive crack signal.

When a single-element horseshoe probe is placed over a crack, the signal output (or detectability in terms of bridge unbalance) is a function of the angular relationship between the flux field and the crack. When the assumption is made that a crack is generally linear, at least over the width of the probe, rotating the probe will produce alignment with maximum crack sensitivity at a twice-per-revolution frequency of the probe. Thus, the output of the bridge becomes an AC crack signal (at two times revolution frequency) superimposed upon a rectified DC proximity signal. With proper filtering (bandpass and low pass), the AC portion is displayed on a read-out device and the DC portion is used to control the gain of the "crack signal (AC) amplifier", thus compensating the gain of this amplifier for variations in proximity while also compensating for general sample surface characteristics such as machining marks and oxidation.

This compensation circuitry was breadboarded and used when feasible during this program, and its effects on compensation are shown on page 12.

SCOPE OF INVESTIGATION

This program has encompassed a 14-month effort performed at Mechanical Technology Incorporated and has included probe design (apparently patentable), a minimum of electronic design devoted to the proximity compensating circuit, vibratory beam fatigue testing, and an added task of examining actual helicopter components returned from field use.

Vibratory beam fatigue tests were run on a minimum of 42 single-element samples (seven groups of samples) manufactured of 6061 T-6 aluminum.

Vibratory beam and low cycle fatigue tests were run on 15 double-element samples comprised of bolted, riveted, and welded configurations.

Control samples were run early in the program and were scanned both by the previous probe and the newly developed one. It became clearly obvious that the rotating probe concept was far superior to the stationary field in determining flaws at an earlier percentage of life of the sample. Thus, the control served as an adequate benchmark in assessing the improvement of the probe sensitivity, as was later borne out by the 42 sample and 15 sample runs of testing.

The samples were not metallographically examined as in the previous contract, since the fatigue damage was induced on identical samples and by the same fatigue testing machines. Thus, the assumption was made that the fatigue damage was similar, and microscopic examination was not necessary. The old and redesigned systems can be adequately compared by examining the results of the fatigue testing, specifically the percentage of life at time of signal.

EXPERIMENTAL METHODS

MATERIALS AND SAMPLE PREPARATION

All of the fatigue testing performed on this contract was concerned with 6061 T-6 aluminum. This material was selected for its somewhat better response with the inductive detection system, its frequency of use in helicopters, and its ease of machining to the various configurations and surface finishes required.

The samples as shown in Figure 1 (#31-36) are examples of the various surface finishes and degradations as called for in the Statement of Work.

Sample #31 is an example of the rough, scratch-brushed group. This surface degradation (as all others) was performed on both sides of the sample, and was relatively uniform from side to side and sample to sample. The scratches ranged up to approximately .010 inch deep.

Sample #32 is an example of the peened group. This surface degradation was performed by peening both sides of the sample to an average depth of .008 inch.

Sample #33 is representative of the as-machined samples, which were bandsawed to size and finished with #80 paper on a belt sander.

Sample #34 is representative of the painted group prior to aging of the paint.

Sample #25 is an example of the vise-pressed group which was placed in a sharp-jawed vise and compressed, leaving the impressions of the vise jaws on the surface. From the fatigue data, a calculated 5-ksi compressive stress was introduced into the surface of these samples. Sample #36 is representative of the anodized samples which were run. The apparent enhancement of the detection system on these samples is discussed on page 24.

VIBRATORY BEAM MACHINES

The vibratory beam fatigue machine is shown in Figure 2. Two of these machines were used in order to facilitate the running of the tests, since the tests required constant monitoring. The dial gage was used during initial setup to measure deflection and to insure a totally reversing stress. An optical sensor was used to measure the actual motion at speed. The difference between the two measurements, which amounted to .002 inch, was then taken into consideration. Therefore, the deflections quoted in the data are actual deflections under dynamic conditions. The machines, which run at a nominal speed of 3450 cycles per minute, were provided with a speed control which allows a small variation in cycle rate to avoid damaging resonances. The total number of cycles was recorded electromechanically.

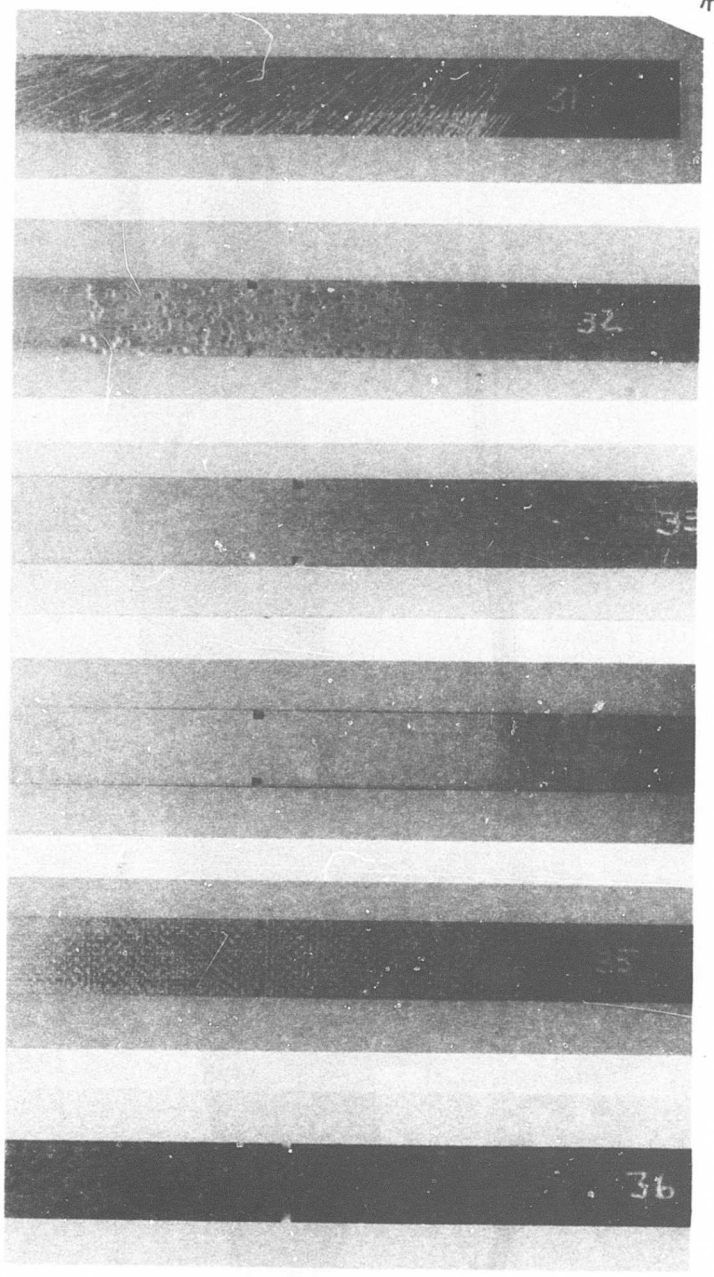

Figure 1. Samples Used.

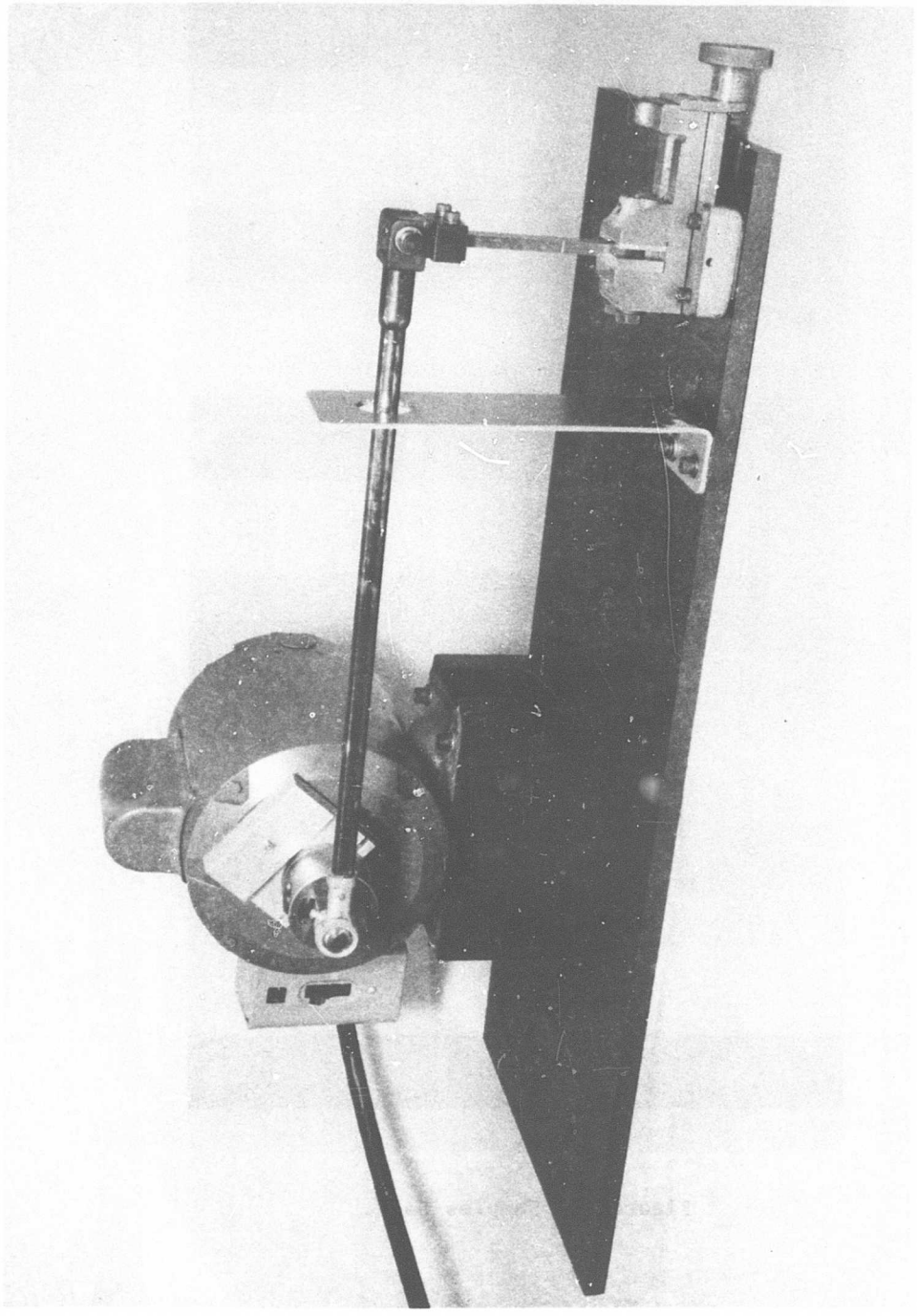

Figure 2. Fatigue Machine.

The sample was firmly clamped in the vise. The upper rod was clamped to the sample, and the system was adjusted to provide the desired positive and negative deflection. The sample was scanned and the test was started. During the initial phases of testing, many inductive scans were taken prior to the first acquisition of a signal; however, with experience, the number of readings prior to signal could be reduced without losing any information. After the first appearance of the signal, readings were taken periodically until failure occurred which we have defined as a fracture.

TEST INSTRUMENTATION

The instrumentation is shown in Figure 3. The probe and a typical sample are on the sheet of paper on the bench. The oscilloscope was used for ascertaining initial bridge balance and for a visual check on the operation of the system. The variable inductor and resistance decade box formed one leg of the AC bridge, and the DC power supply provides the motor drive voltage for the rotating probe. The bottom rack contains the 50 KHz oscillator, its power supply, and the demodulator (as used in the previous work). The electronics rack contains two variable filters which are arranged to form a narrow bandpass at the two-per-revolution frequency of the probe. The analog AC voltmeter provides a visual crack indication to the operator of the system. It also provides a 0-1 volt DC analog output which we have used to drive the recorder shown and a Roback digital voltmeter from which the reported data was read.

The operator balances the bridge while holding the probe against a good portion of the sample and adjusting the inductance and resistance for a null on the oscilloscope. The probe is then scanned over the specimen while watching the AC voltmeter. Any crack or linear flaw passed over by the probe will generate a twice-per-revolution modulation which can be seen on the oscilloscope, demodulated and filtered, and read out on the analog or digital voltmeters. The typical background seen on the analog voltmeter is less than 0.01 volt, while our standard crack signal (1F) is seen as 0.85 volts. This crack is not visible under a 10X glass and, as can be seen from microscopic examination, is a beginning crack.

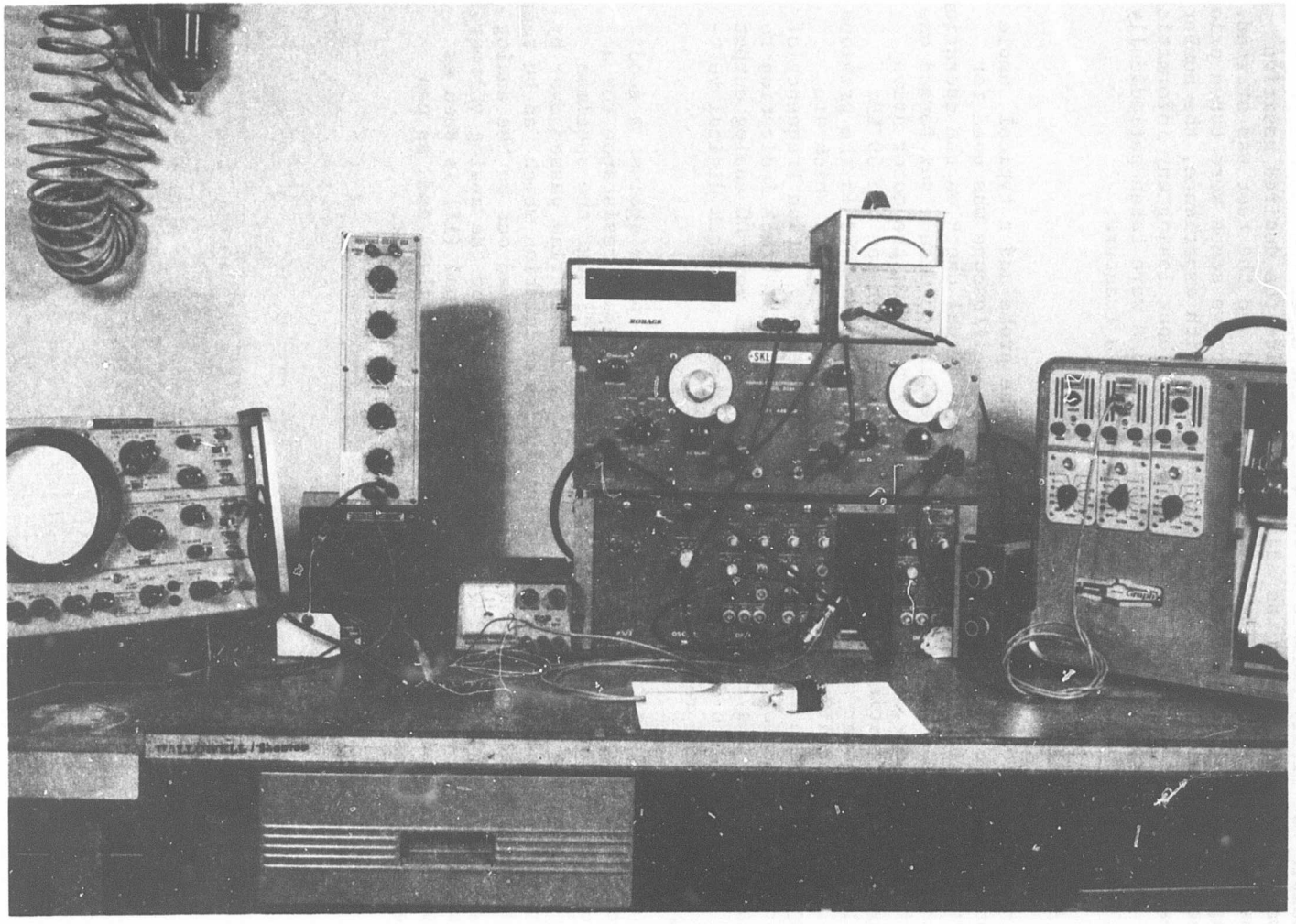

Figure 3. Laboratory Test Instrumentation.

RESULTS OF PRELIMINARY DESIGN STUDIES

The objective of Task I - Redesign - was to reduce the effects of such variables as specimen surface condition, geometry and proximity, on the effectiveness of the inductive sensing system in the detection of fatigue cracking. A number of approaches were considered at the inception of the program, and a logical development effort eliminated all but the most feasible from the standpoint of both laboratory and field utilization.

A linear array of axially symmetric probes was considered and found wanting. The effects of proximity and surface condition could be compensated for by use of "dummy" probes in the array; however, this configuration would severely restrict the geometries which could be examined just due to the size of the array. In an effort to minimize the size of array, a four-coil probe was built and evaluated. Figure 4 shows three views of the four-coil configuration.

The four-coil configuration allows good compensation so that lift-off and tilt sensitivity are minimized. A feature of the four-coil arrangement is that a greater area of sample may be scanned without sacrifice of sensitivity due to the enlargement. The four coils are arranged such that their axes are perpendicular to the sample and are positioned at the corners of a square some .4 inch on a side. Due to the construction of the core and the uniformity inherent in the ferrite material (as opposed to a wire core), very good lift-off compensation has been obtained. This type of probe could prove very useful when large areas of a specimen are to be examined.

As discussed under Theory of Operation, the basic element in the probe system is a horseshoe-shaped core around which the winding is placed. A single horseshoe and double horseshoe were investigated in the previous contract and were finally abandoned in favor of an existing axially symmetric (multiple leg horseshoe) probe due to the directionality effects; i.e., a crack at 45° to the flux path gives a different signal than the same crack at 90° to the flux path. This directionality became an asset in that crack sensitivity was increased while proximity effects were minimized.

Figure 5 shows a "horseshoe" probe configuration where the core has been fashioned by slotting a ferrite bead. A 200-turn coil is wound on this bead, forming a probe. The crack sensitivity of this probe is superior to that of the previous probes; however, the probe is directional and is quite sensitive to lift-off. To eliminate this unwanted characteristic, the probe is rotated with respect to the specimen where the signal is now seen as a twice-per-revolution "pip" which occurs at the rotating frequency. This rotation offers significant improvements in the probe operation:

1. The signal appears as an AC signal at two times rotational speed, thus allowing narrow band filtering to minimize noise.

2. Lift-off of the probe will cause a variation in the output at such

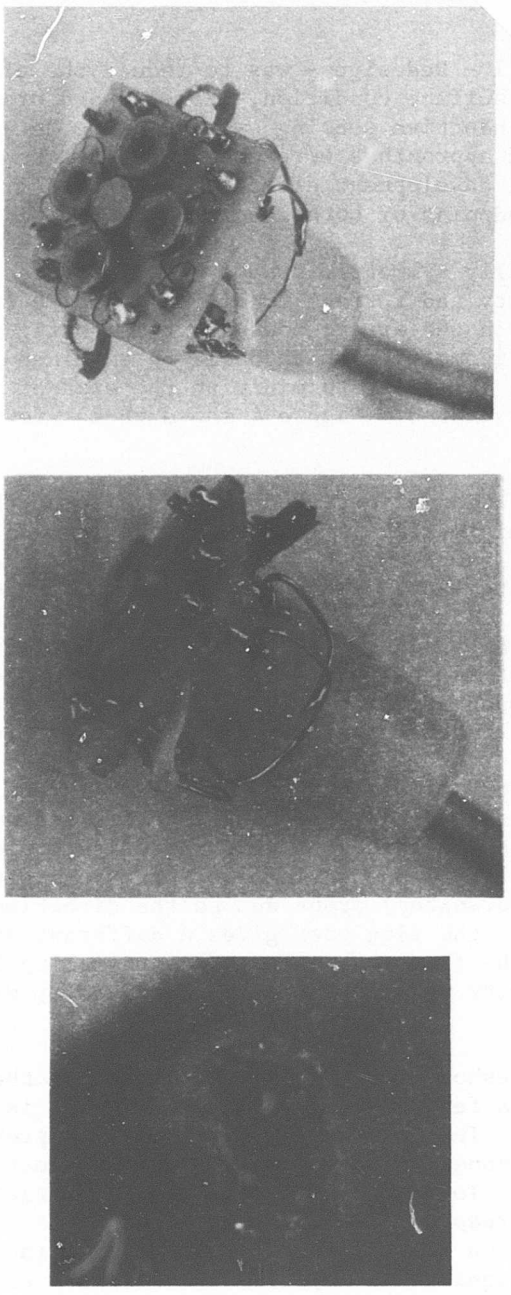

Figure 4. Four-Coil Probe.

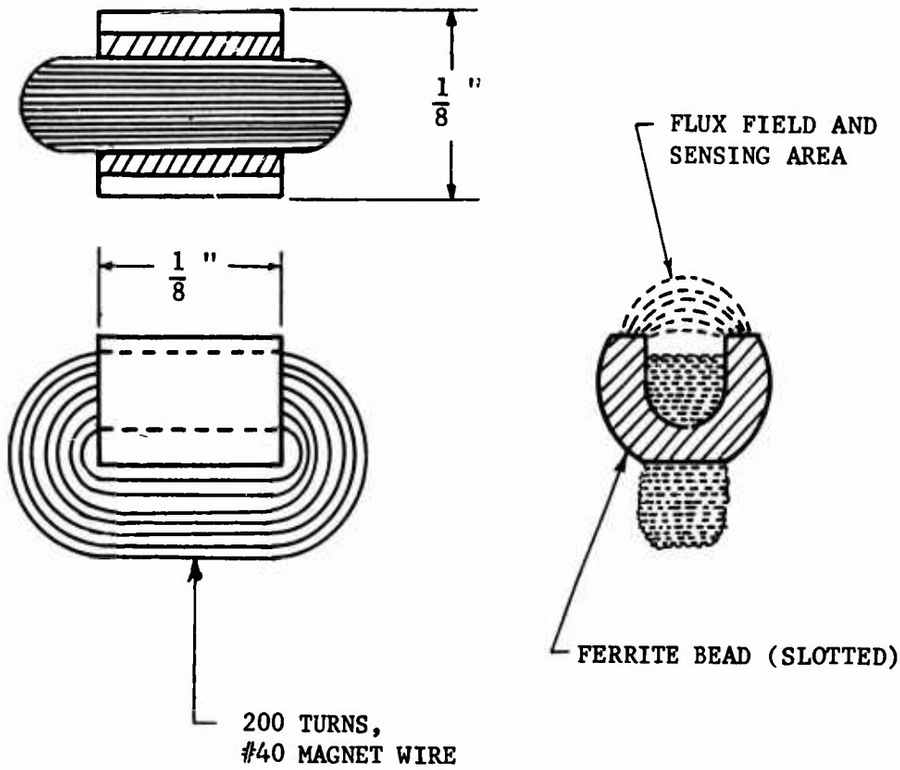

Figure 5. Sketch of Ferrite Bead Probe.

a low frequency (essentially DC) that it would not be seen.

3. The directionality of the probe actually enhances the sensitivity and improves the S/N ratio.

Figure 6 shows the overall laboratory test setup, while Figure 7 shows a detail of the probe and sample arrangement (in this case the sample was rotated rather than the probe). The probe indicated at the end of the probe holder is the one in the sketch.

An additional, very important benefit is that the "lift-off signal" may then be used to automatically adjust the gain in the "crack signal" amplifier and thereby obtain a degree of compensation for changes in crack sensitivity due to variations in lift-off; i.e., at large lift-off spacing, the gain of the crack signal amplifier will be increased. This also minimizes the effects of "roughness", paint, grease and oil, oxidation and anodizing, as required in the Work Statement of this contract. This concept is shown in the block diagram of Figure 8. This is a significant advance over other crack detection systems which cancel the effect of lift-off variations but provide no compensation of the crack sensitivity changes due to these same lift-off variations. An additional benefit of the rotating probe is that a crack is detected regardless of its orientation; whereas with a crossed coil arrangement, cracks passing at 45° to the axis of the coils will not be detected.

The first experimental rotating probe assembly incorporating slip-rings and a miniature DC motor to rotate the MTI horseshoe inductive probe was built and evaluated. Figure 9 shows this device with the slip-ring shield and "nose cone" removed. The horseshoe probe is visible at the end of the assembly. The slip-rings and brushes connect the rotating probe to one of the cables, which in turn connects to the electronic systems used to excite the probe and amplify its signal. The other cable is used to supply DC current to the motor.

Figure 10 shows the device with the slip-ring shield and nose cone installed. The nose cone projects approximately 10 mils beyond the end of the rotating probe. Thus, when the nose cone is held in contact with a sample surface, the probe rotates with a 10-mil gap between itself and the surface being inspected.

Figure 11 is a plot of the DC output voltage versus air gap (or standoff distance) for this device when being "driven" by the existing electronics and with the probe stationary. Figure 12 shows the angular crack sensitivity at .000 inch, .005 inch, .010 inch, .020, and .030 inch standoff distance.

These two curves show that the "horseshoe" probe has a relatively constant crack sensitivity over a range of standoff distance considerably larger than what could be expected due to surface variables such as roughness, paint, grease and oil. Figure 13 is a recording taken at the raw output of the electronics with the probe rotating and passing over a microcrack.

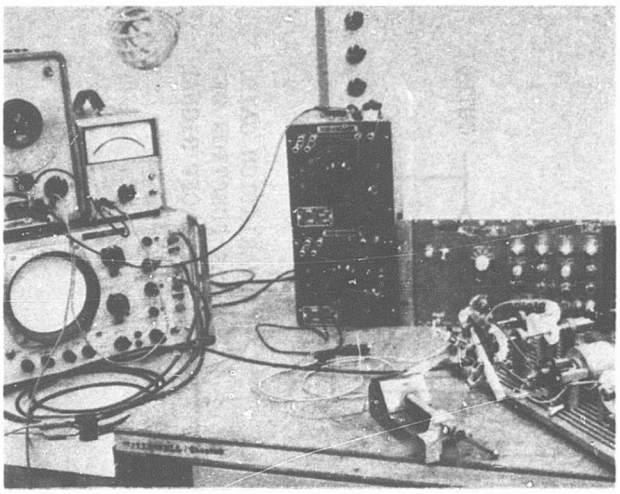

Figure 6. Test Setup for First Rotating Probe.

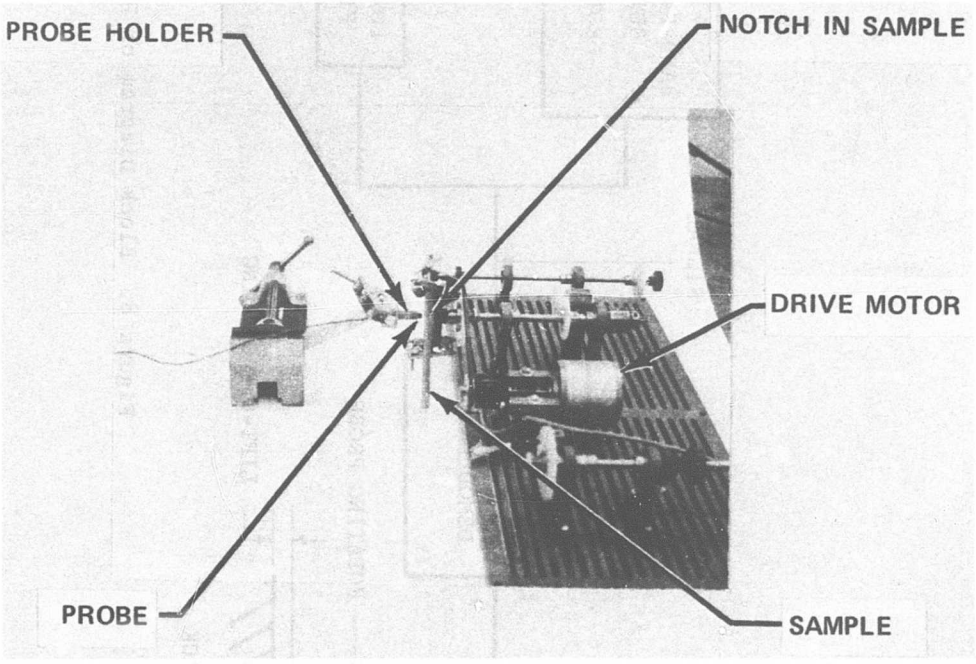

Figure 7. Detailed Photograph of Probe and Sample.

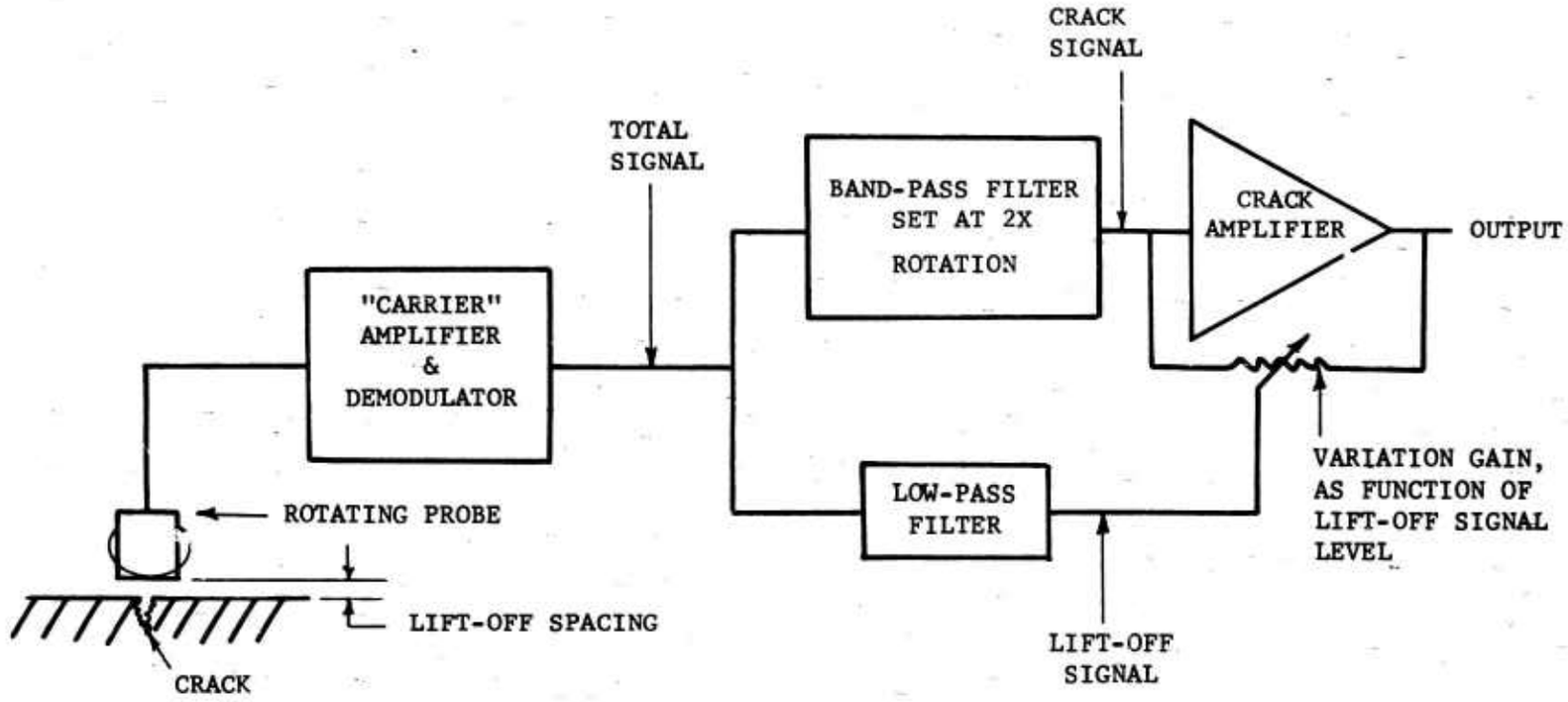

Figure 8. Block Diagram of Probe System.

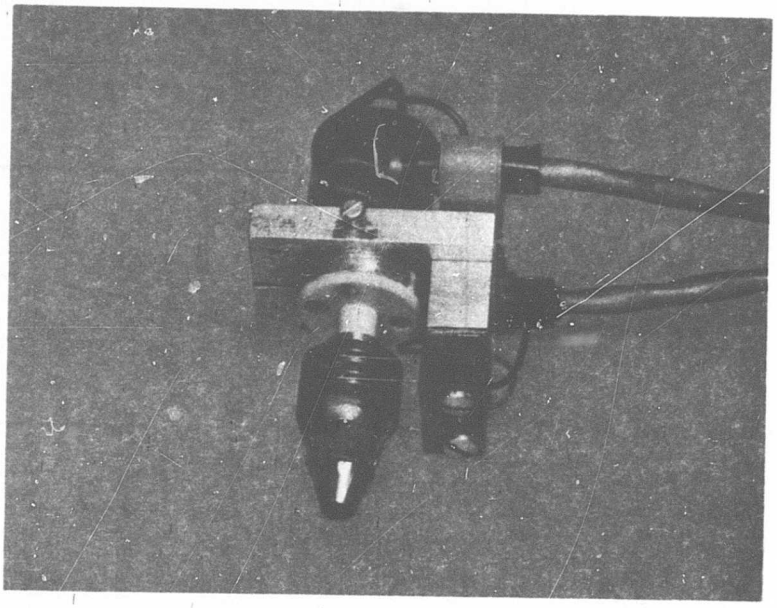

Figure 9. First Rotating Probe.

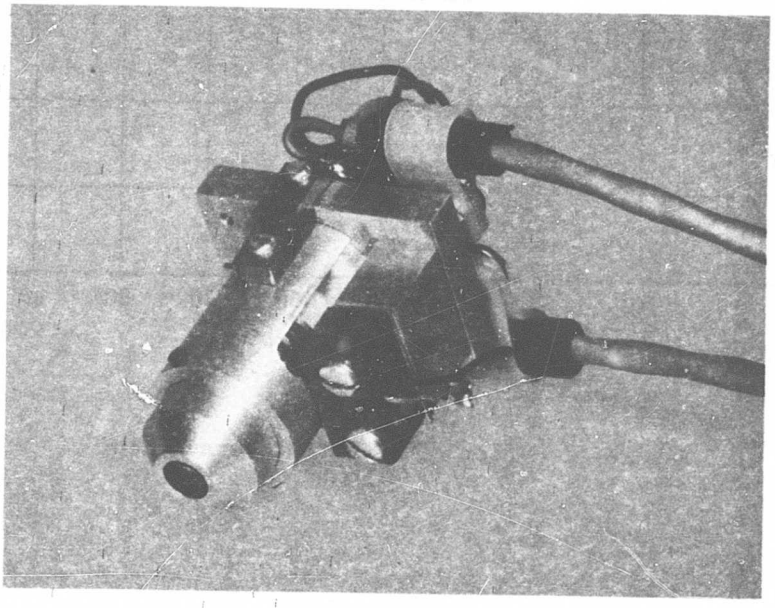

Figure 10. First Rotating Probe With Shield.

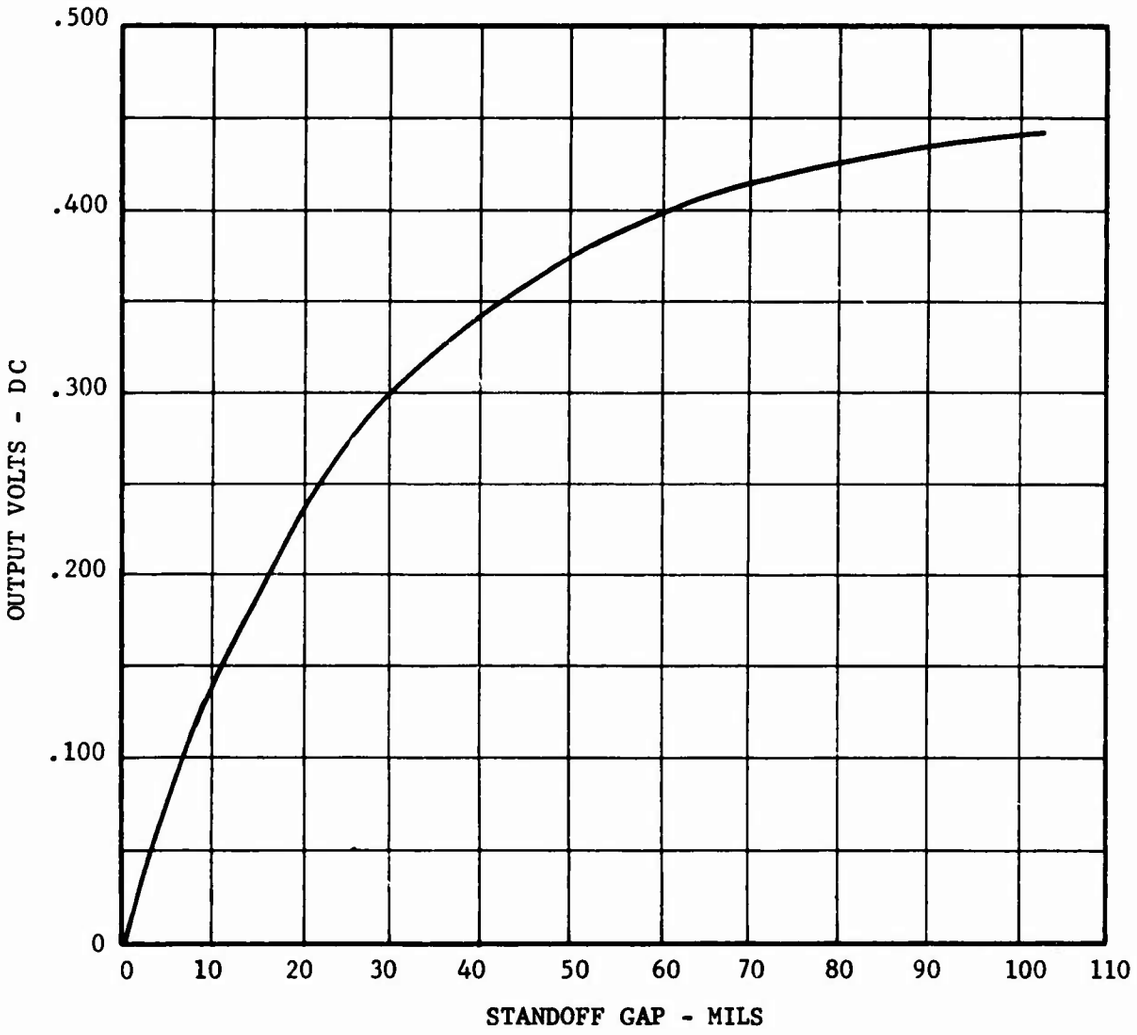

Figure 11. Plot of DC Output Versus Gap.

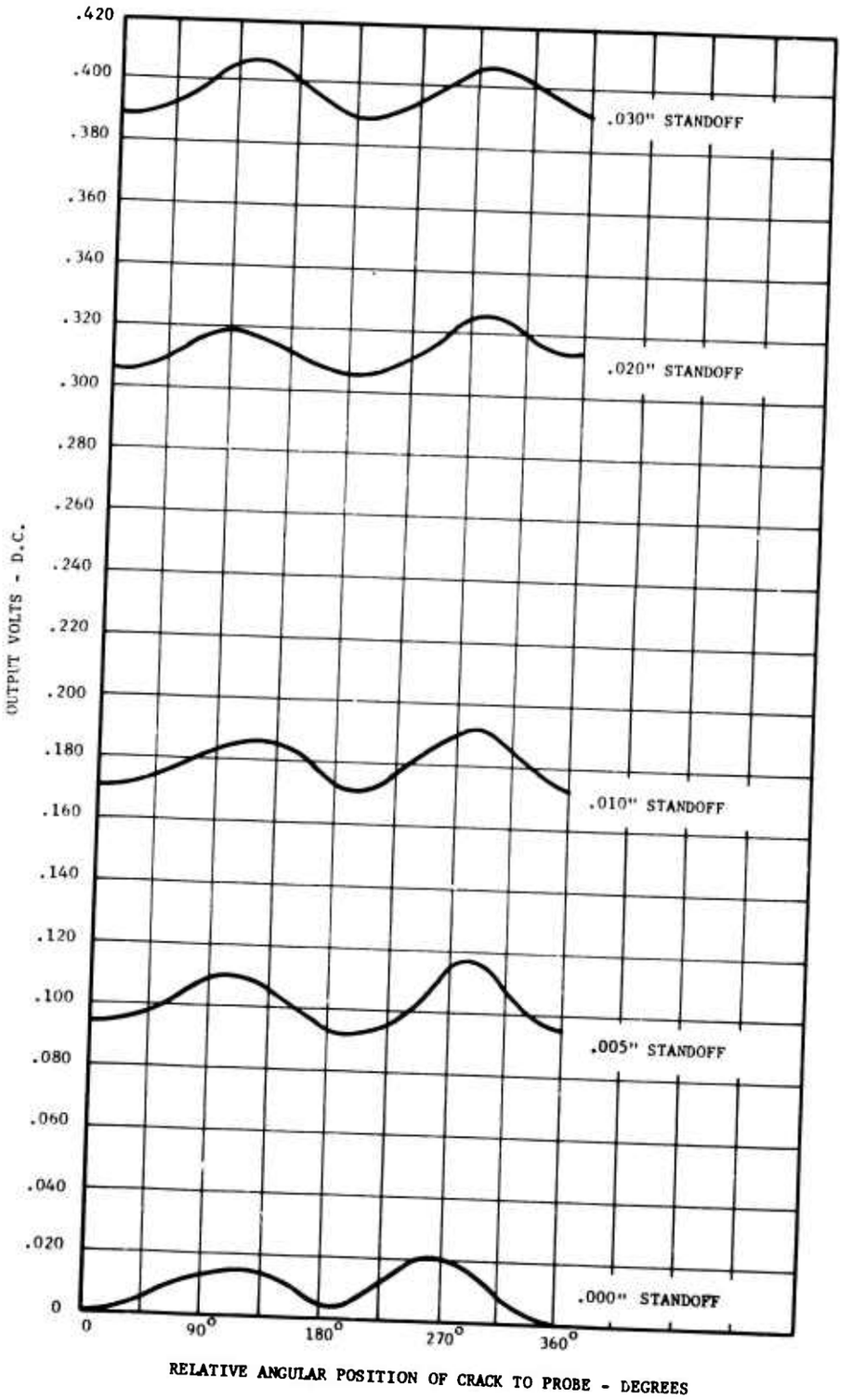

Figure 12. Plot of DC Output Versus Gap for Various Standoff Distances.

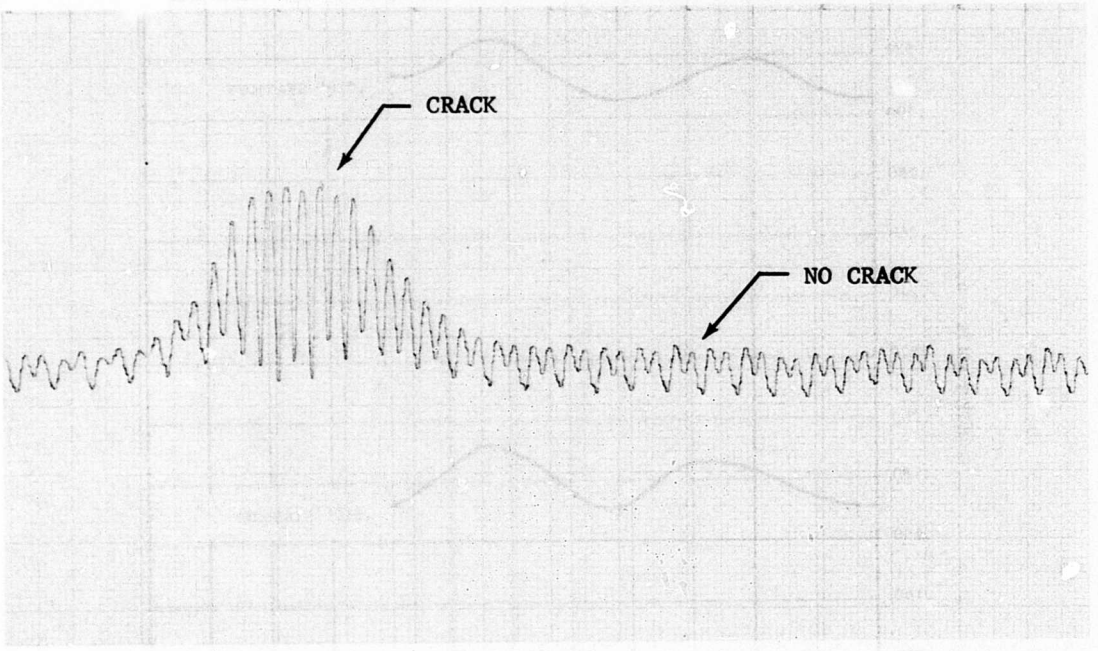

Figure 13. Chart Recording of Raw Crack Signal.

This recording was taken on sample 1F, which was one of the control samples. The trace is composed of a carrier at approximately 26 Hz which is modulated by the crack signal. The 26 Hz carrier is filtered out in the subsequent electronics, and the S/N ratio is enhanced by utilizing the DC proximity signal to control the amplification of the crack signal, thereby achieving the 85 x S/N ratio noted on page 7. To relate this signal to percentage of life (used up), we may compare the 85 x S/N ratio against the data for the similar samples and arrive at approximately 60% of life. Since normal criterion for a first crack signal was 2 to 3 times background, the signal in Figure 13 indicates a crack of considerable size.

The second rotating probe assembly was constructed for use in the fatigue testing portion of the contract. This was an entirely new assembly which included a precision, miniature motor and miniature gold alloy slip-ring and brush assembly. These are visible in Figure 14, which shows the assembly with the aluminum extension removed. The mu-metal magnetic shield surrounding the inductance probe is also shown in the figure. This unit operates very smoothly and quietly, and the overall signal-to-noise ratio when detecting the microcrack in the aluminum reference sample 1F is in the order of 100:1.

Figure 15 is a plot of the DC output voltage versus standoff gap of experimental prototype #2, and Figure 16 is a plot of the crack sensitivity versus standoff gap, as read on the AC millivoltmeter at the output of the electronic filter when examining the microcrack in aluminum sample 1F.

It will be noted from Figures 11 and 15 that prototype #2 has a smaller linear range than prototype #1, but was judged necessary in order to reduce the effects of stray fields. The magnetic shield also restricts the sensing field to the area directly in front of the rotating ferrite bead. This is beneficial in that the probe can scan areas very close to discontinuities such as edges, joints and rivet heads.

The second experimental rotating probe, described above, was operated for approximately 100 hours during a preliminary testing period. The unit continued to perform well, with the gold alloy slip-rings showing very little signs of wear. The system was successfully operated without the twice-per-revolution electronic filter described previously. This is due to the fact that the system noise level, even without filtering, is in the order of 40:1 and can, therefore, still easily detect cracks. Absence of the filter causes slightly more noticeable transient signals to appear due to rapid changes in standoff distance, but this is not judged to be a significant problem at this time. Removal of this filter simplifies the electronics and eliminates the need for operating the drive motor at a constant speed. The filter was used for all of the fatigue testing data.

The penetration depth in aluminum of this probe is approximately .015 inch, and the width of the sensitive area is approximately 9/32 inch. Metallographic examination was not performed rigorously as in the previous program; however, the present probe is clearly more sensitive as seen by the earlier appearance of signal during fatigue testing. The minimum crack

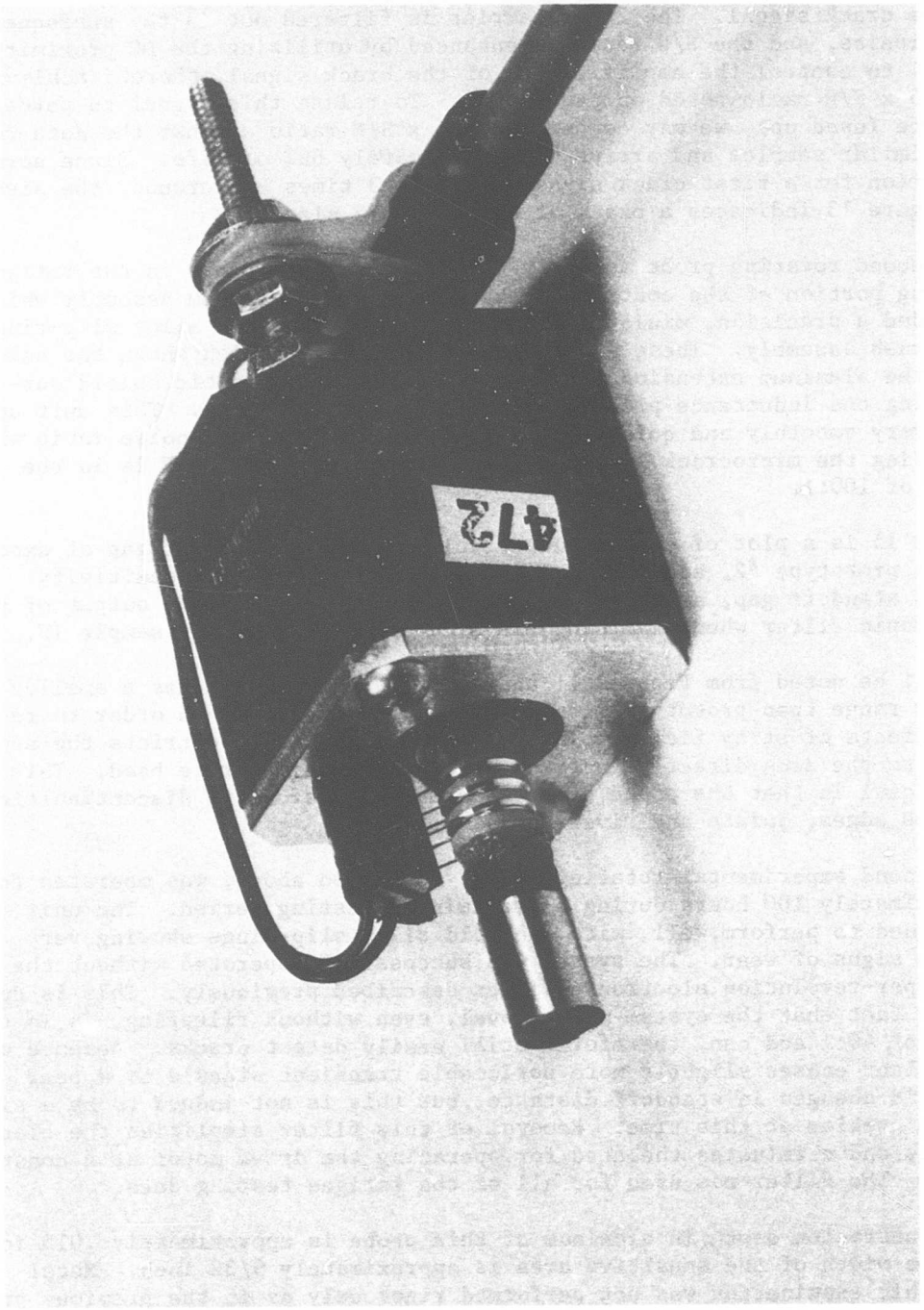

Figure 14. Detailed Photograph of Second Rotating Probe.

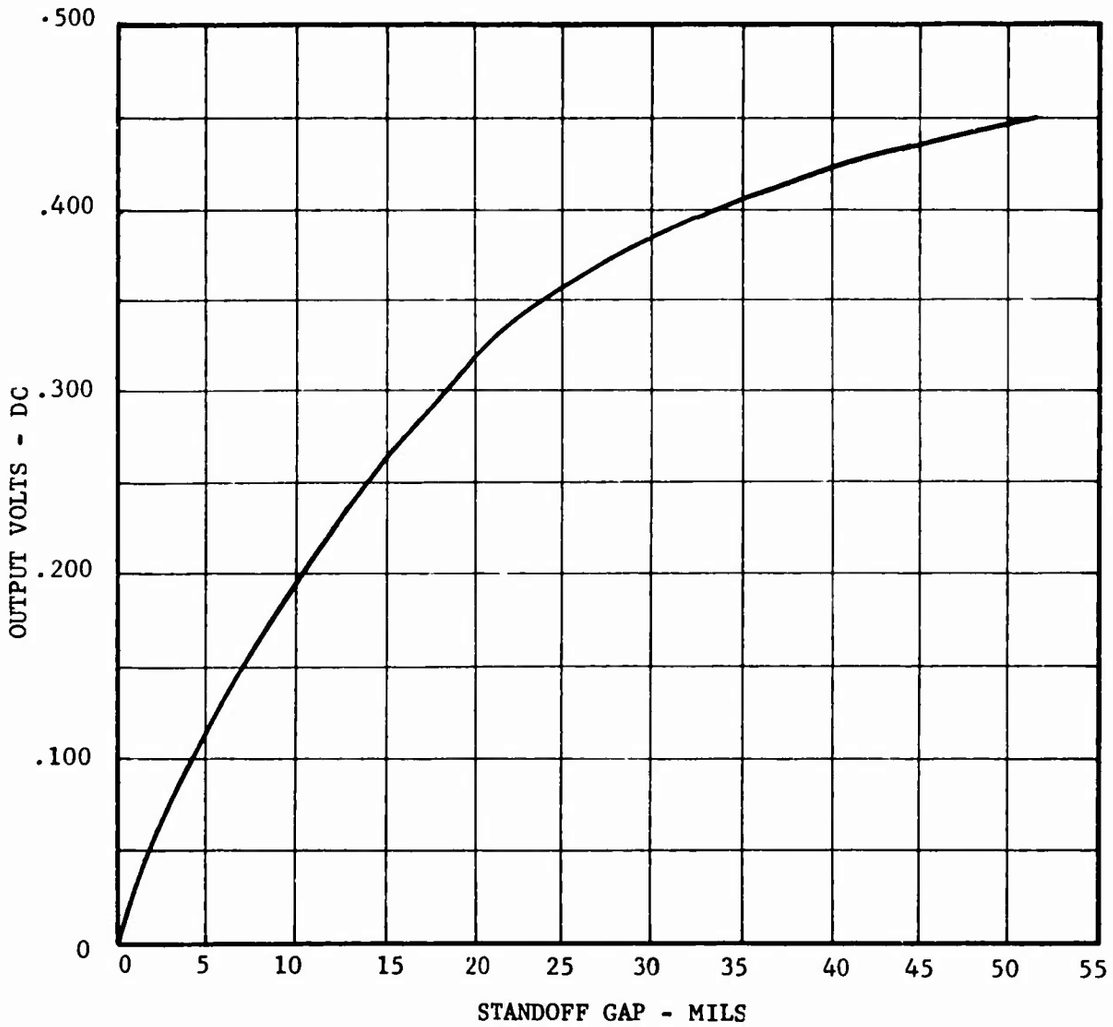

Figure 15. Plot of DC Output Voltages Versus Gap.

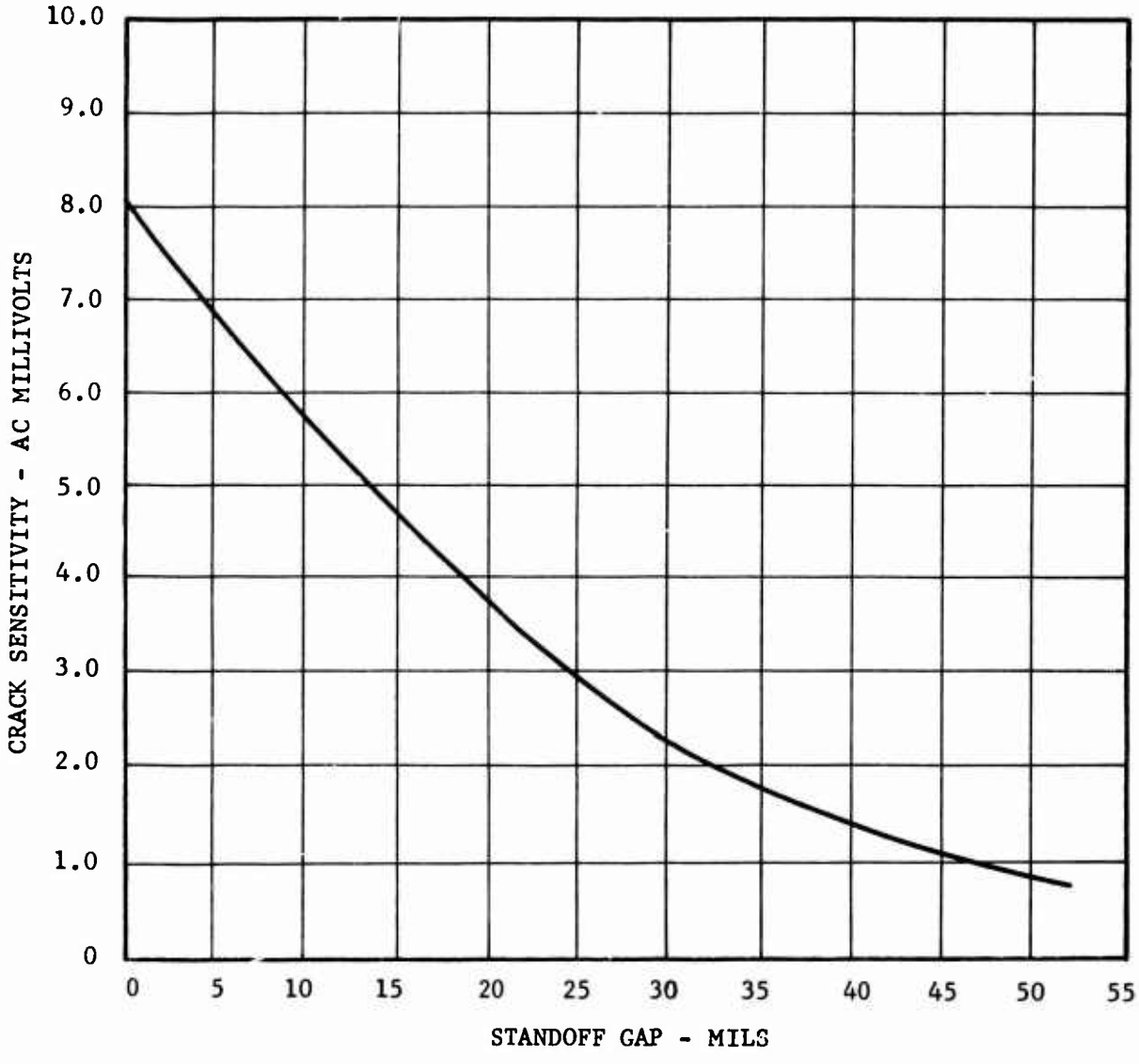

Figure 16. Plot of Crack Sensitivity Versus Gap.

size detectable by the previous probe was in the 10-microinch range, and it is inferred that the present probe performs at least as well.

The effect of tilt (deviation from perpendicular) is quite low as long as the angle remains below approximately 20°. This has been demonstrated in our preliminary experimentation and testing program. The probe is set over the crack and the crack reading obtained. The probe is then tilted and the drop in reading observed. Typically a drop of 5-10% of reading is seen which does make the crack appear "smaller", but does not affect the ability to find it as long as the 5-10% drop in signal does not drop the reading to background.

The rotating probe was tested briefly with titanium. Since no cracked titanium was available, a crack was simulated by butting two machined surfaces together. The crack sensitivity was approximately one-fifth that obtained with aluminum, but is still well above the system noise level.

RESULTS OF EXPERIMENTATION

VIBRATORY BEAM FATIGUE TESTS

The first group of samples run for the testing program was fabricated to the configuration shown in Figure 1. The specimens were scanned so that the edge of the sensitive area of the probe just missed the end of the notch. With this scanning geometry, a crack initiating from a corner of the notch would be seen early in its life. The results of these samples (200-205) are as follows:

	Cycles		
Sample	Signal	Life	Percent of Life
200	100K	1033K	10
201	100K	656K	15
202	300K	1160K	26
203	200K	621K	32
204	300K	694K	43
205	400K	1064K	38

Using percentage of life at time of first acquisition of signal as a figure of merit, the first group of samples shows 27.3% as an average, with a spread from 9.7% to 43.2%. In order to compare these results with results shown in previous work, the center of the sample was also scanned. This percentage is, of course, greater due to the propagation of the crack from the notch to the center of the sample, and averages out at 61.7% with a spread from 30.5% to 64.4%. These first samples received no special surface preparation and were run as machined.

The second set of samples was given a black anodize treatment and run in the same manner as the previous one. These six samples showed an average of 19.4% life at time of signal with a spread of 11.9% to 20.8%.

	Cycles		
Sample	Signal	Life	Percent of Life
206	200K	958K	21
207	100K	754K*	13
208	250K	1322K	19
209	150K	1156K	13
210	130K	1086K	12
211	130K	982K**	13

*Broke between vise and notch
**Broke at vise

The anodizing process produced two interesting anomalies in the testing results:

1. The hard surface layer appeared to initiate cracks at areas away from the notch.

2. The percentages were more tightly clustered, and the overall average is lower.

The anodize process forms a hard and relatively brittle surface on the sample, and this surface layer is very well bonded to the substrate. Consequently, a large number of cracks can form in the anodized surface layer and then proceed to propagate into the specimen material. Sample 211 broke at the vise which forms the lower support for the fatigue samples, and is an occurrence which has not been unusual in our fatigue testing. This is due to the fact that the notch is not always the most significant stress raiser in the given sample configuration.

The conclusion to be drawn from samples 207 and 211 is that the samples would have run longer before they failed at the notch, thus reducing the percentage of life at time of signal.

The third set of samples was vise-pressed as shown in Figure 1 (#35). This operation damaged the surface by leaving impressions of the vise jaws in the surface of the specimen. Since a significant (calculated 5 ksi) compressive stress was introduced, deflection had to be increased in order to produce failure in the order of 1 x 10^6 cycles; the results are as follows:

	Cycles		
Sample	Signal	Life	Percent of Life
212	800K	2748K	32
213	800K	1949K	41
214	150K	400K*	37.5
215	300K	802K	37.4
216	160K	540K*	29.7
217	150K	862K	17.4

*Broke at vise

These six samples showed an average of 32.5% life at time of signal with a spread from 17.4% to 41%.

The fourth set of samples run was of a different configuration such that the stress raiser was a curved, necked-down cross section in the sample, and the probe was scanned along the inside radius. The average percentage of life at time of signal was 72.5, with a spread from 61.5% to 89.6%. The late appearance of these signals is due to the fact that the stress raiser was no longer a milled or sharp-cornered notch as in the other samples, but a comparatively larger radius, i.e., a standard method of increasing fatigue life in design of structural members. The data are as follows:

	Cycles		
Sample	Signal	Life	Percent of Life
218	830K	1026K	80.9
219	2000K	3250K	61.5
220	450K	680K	66.2

221	1225K	1367K	89.6
222	876K	1196K	73.2
223	350K	489K	71.6
224	725K	1120K	64.6

The fifth set of samples was machined to the standard, notched configuration, painted with a variety of paints, and aged by baking and overbaking, thus producing a poor-appearing painted surface, simulating old paint.

The average life at time of signal was 32.7%, with a spread from 23.7% to 40.7%. The data is as follows:

	Cycles		
Sample	Signal	Life	Percent of Life
226	300K	781K	38.4
227	250K	1055K	23.7
228	300K	1124K	26.7
229	400K	1047K	38.2
230	250K	873K	28.6
231	350K	859K	40.7

The sixth set of samples was of double-element welded configuration, with a butt weld. The 1/4-x-1/2-x-5-inch sample was cut, beveled, and welded back to 1/4-x-1/2-x-5-inch size. The weld area was belt sanded to approximately original dimensions. No notch was cut in these samples, since it was assumed that the weld was a sufficient stress raiser to force failure to occur in the heat-affected zone. This was not always the case, as a few of the samples tested broke at the holding vise. This problem was circumvented by removing the samples and also scanning them in the area of the vise closure. This approach yielded good data:

	Cycles		
Sample	Signal	Life	Percent of Life
233	1550K	2202K	70.4
234	350K	674K	51.9
235	200K	686K	29.1
236	1300K	1518K	85/6
238	1000K	2146K	46.5
239	500K	1882K	26.5

The average percentage of life at time of signal for these tests was 51.7, with a spread from 26.5% to 85.6%.

The seventh set of samples run consisted of a 1/4-x-3/4-x-5-inch beam sample with a drilled hole 2 inches from the bottom end. This was done to investigate the ability of the inductive system to detect cracks in the vicinity of attachment holes. The data are as follows:

Sample	Cycles — Signal	Life	Percent of Life
250	150K	738K	20.4
251	150K	320K	47.0
252	150K	723K	20.8
253	100K	700K	14.4
254	400K	830K	48.2
255	400K	863K	46.4
256	300K	968K	31.0
257	250K	921K	27.0

Samples 254 and 255 were manufactured to the above configuration; however, a round-head aluminum rivet was inserted in the drilled hole. The percentage of life at time of signal is higher due to the fact that the crack initiated under the head of the rivet, and the probe was not able to detect the crack until it had propagated beyond the rivet head. Samples 256 and 257 were run with a countersunk hole into which was inserted a flat-head aluminum rivet. Again the crack was detected after it had propagated beyond the head of the rivet; hence, the greater percentage of life at time of signal.

Samples 258-263 were surface damaged by peening as in Figure 1 (#32). Since a significant body of data existed on the notched configuration, these samples were not fatigue cycled but were scanned to determine the effect of the surface degradation on background signal. The background signal increased slightly but not more than 25% on any sample, while the crack criterion for first appearance of signal has been at least 100% above background (2:1) and in most cases 4:1 or 5:1 during our testing phase.

Samples 264-269 were scratched as in Figure 1 (#31). These samples were treated in the same way as samples 258-263 in that they were not fatigue cycled but were carefully examined for increase in background signal. As above, no more than 25% increase in background signal was observed, and on this basis, it was determined that the overall system's crack detection capability was not significantly affected.

The remaining double-element samples were not of a configuration that could be readily run in the available fatigue machines and, therefore, were subjected to low cycle bending tests as provided for in the Statement of Work. Three samples were lap welded and bent to determine the ability of the probe to examine the fillets on each side of the lap.

It was observed that the fillet (1/4 inch radius) was small compared to the length of the flat nosepiece of the probe (see Figure 17), and consequently, the angle between the probe surface and the weld varied greatly as the probe (with its motor) was scanned across the weld. No problem was experienced when scanning the flat portion of the specimens. The 1-inch cube motor set approximately 1 inch back from the probe face prevented the operator from placing the probe face close enough to the weld edges to obtain a meaningful reading. This indicates that in future

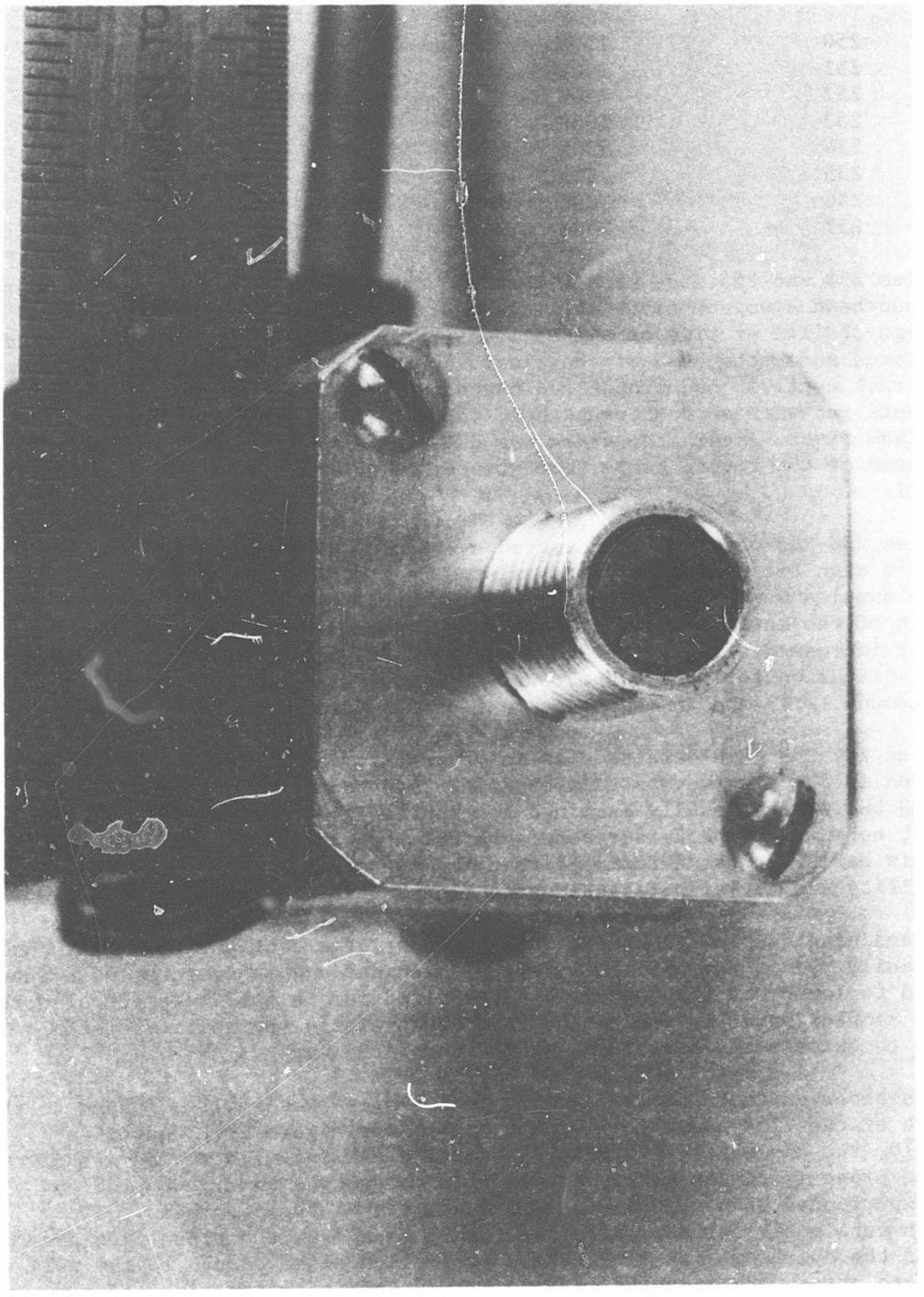

Figure 17. Nosepiece of Probe.

designs the motor should be either smaller or set back from the probe to allow a very small probe head to examine small internal radii. External radii present no serious problems in that the probe can be placed close enough to the specimen to allow meaningful examination.

Three bolted samples were assembled and subjected to low cycle bending tests. The cracks which appeared were located by the inductive sensing system prior to their appearance visually. The cracks were located as in the riveted samples, in that the crack originated under the bolt head and nut, and were not detected until sufficient propagation had taken place and the crack extended beyond the head of the fastener.

Three samples were assembled as above; however, the fasteners were rivets. The same observations apply, in that the crack was detected when it had propagated beyond the head of the rivet.

The remaining requirements for the program had to do with insensitivity to grease and oil on the surface of the specimen. This total insensitivity was shown during the design phase of the program, where there was no measurable deleterious effect on the performance of the probe system. Due to the fact that the rotating probe tip was exposed, it would not have been wise to expose the probe and slip-rings to excessive amounts of grease and oil such as would have been the case had a series of samples been fatigue cycled and scanned repeatedly. With the proximity compensating circuit, a thin foil or insulating material can be placed over the rotating probe to protect it.

SCANNING OF ACTUAL COMPONENTS

A number of helicopter components were received from Eustis Directorate for examination using the inductive sensing system. These included portions of aluminum-faced honeycomb skin, turbine blades, a turbine rotor and stator. These components were inspected and scrapped at the ARADMAC facility due to obvious failure. The circular components were set up on a rotating table, and the probe was positioned over them as shown in Figures 18 and 19. The obvious cracks were generally separations at or around welds in the vicinity of the blades and were quite wide (pencil lead width in one case); they were seen by the inductive sensor. Another typical flaw is seen clearly in Figure 19 as a vertical crack from a weld to the edge of the assembly. Hand scanning located these cracks where they were accessible externally; however, the probe and motor assembly proved too large to be able to scan internal areas such as between blades. The circular scanning (as pictured) on one of the disks showed a number of points which could have been early indications of impending cracks. The background level was quite high on this disk due to severe erosion, and visual inspection was impossible; however, there were readings of three times background, which would normally indicate a flaw. A careful examination was performed on all of these areas using a dye-penetrant technique, and no flaws were indicated. This observation, in the light of previous comparisons run between the inductive system and dye-penetrant, would indicate that the flaws are extremely small at the time of inspection and the penetrant lacks sufficient sensitivity to

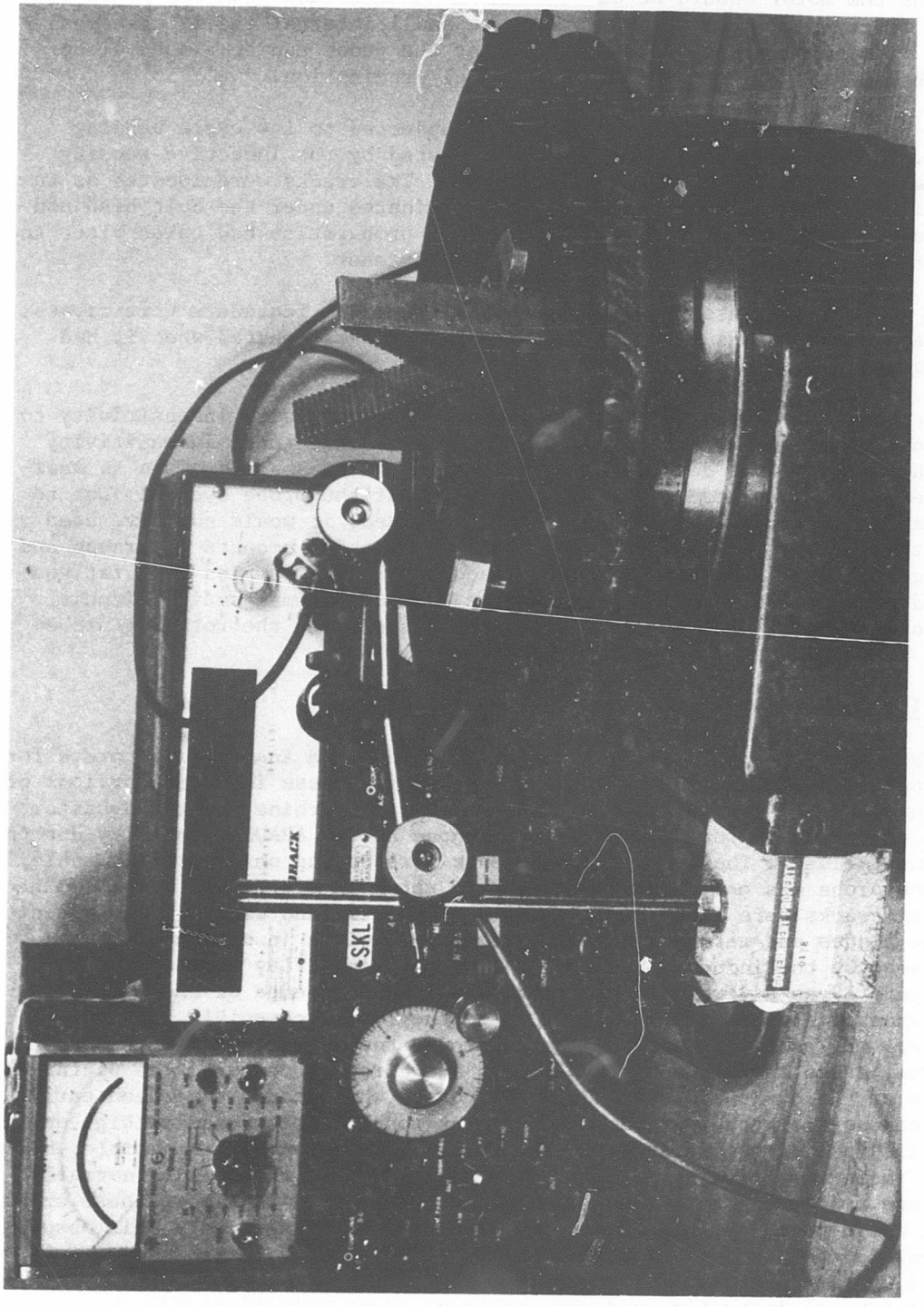

Figure 18. Test Setup for Helicopter Components.

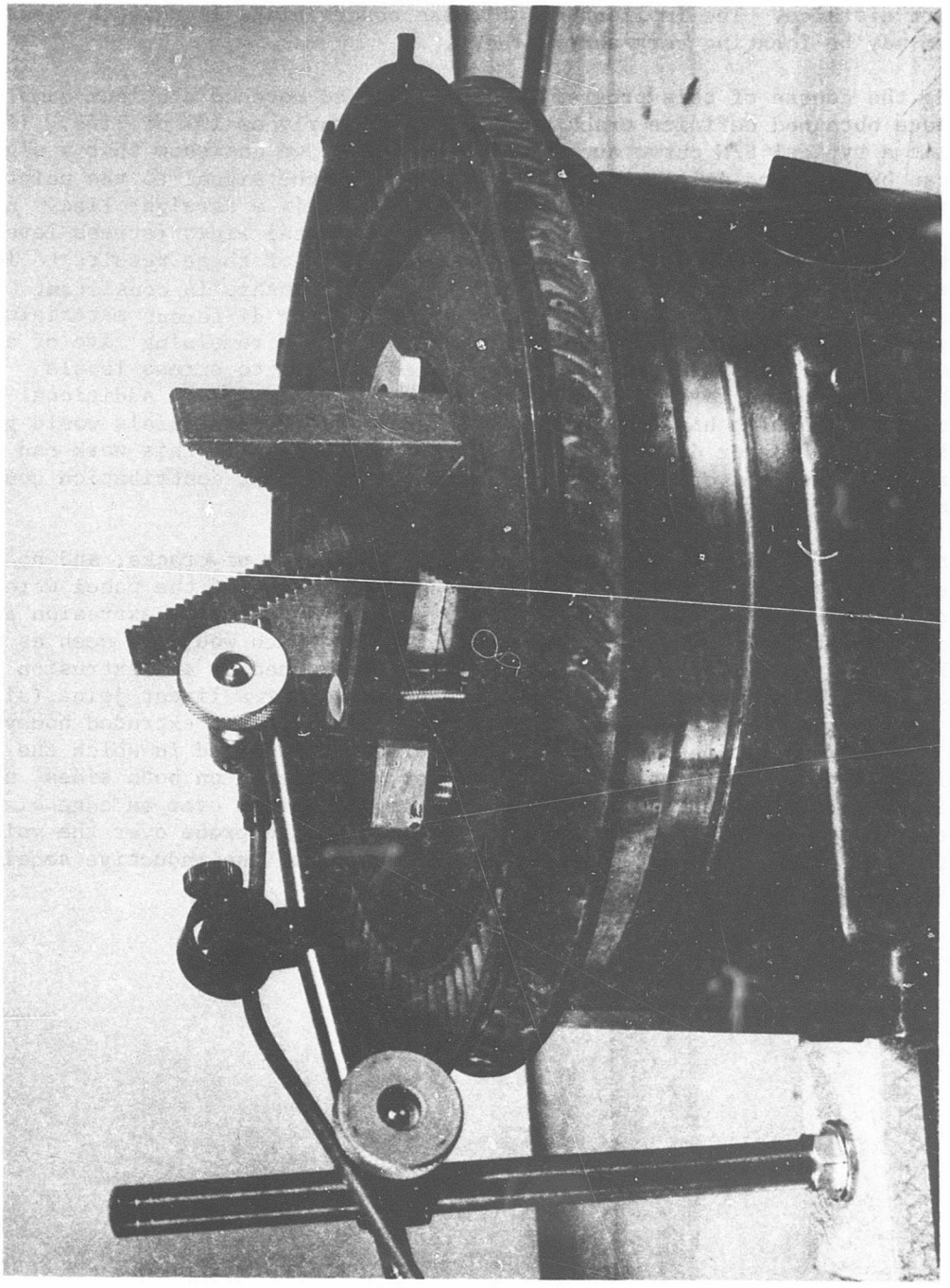

Figure 19. Detailed Photograph of Scanning Method Used for Helicopter Components.

make them visible. In order to definitively find the reasons for these signals, the samples would have to be polished, sectioned, and metallographically examined. These signals were significant in amplitude (approximately 3 times background), and some were able to be followed radially for a short distance. The implication of these observations is that the sensing system may be locating very early cracks.

During the course of this program, we have scanned notched aluminum samples and have obtained definite crack indications as early as 10% of life. If we plot a typical S/N curve such as in Figure 20, we can show that a signal can be obtained at point x, and the growth of the signal to the point of failure plotted as log V versus N is approximately a straight line. At this point, we hypothesize that a family of horizontal lines (stress levels) can be drawn on this curve to extend the usefulness of these results to low cycle fatigue damage. If the log V versus N relationship is consistent among various materials, a point could be defined for different materials and stress levels which would be an indication of the remaining life of a structure. Our present work has been limited largely to stress levels which would produce failure at approximately 1×10^6 cycles. Additional experimentation with higher stress levels and different materials would go far toward proving or disproving the above hypothesis. If this work can be extended to the area of low cycle fatigue, a significant contribution could be made in the prediction of remaining life.

The honeycomb panel sections were scanned for evidence of cracks, and no cracks were noted. The extrusions of the aluminum face of the panel were of such depth that the sensing system showed the edges of the extrusion as an edge of material, i.e., a linear discontinuity which would be seen as a crack. The aluminum honeycomb portion which was bonded to the extrusion was of the size of the probe and thus presented either a linear joint (signal) or background. Thus, the application of the probe to extruded honeycomb panels is questionable. Two flat panels were received in which the aluminum was the honeycomb material; however, the facing on both sides was a dielectric. The result was that positioning the probe over an edge of the comb produced a linear signal, and positioning the probe over the void produced a low background. Again, the application of the inductive sensing system to such panels is of questionable value.

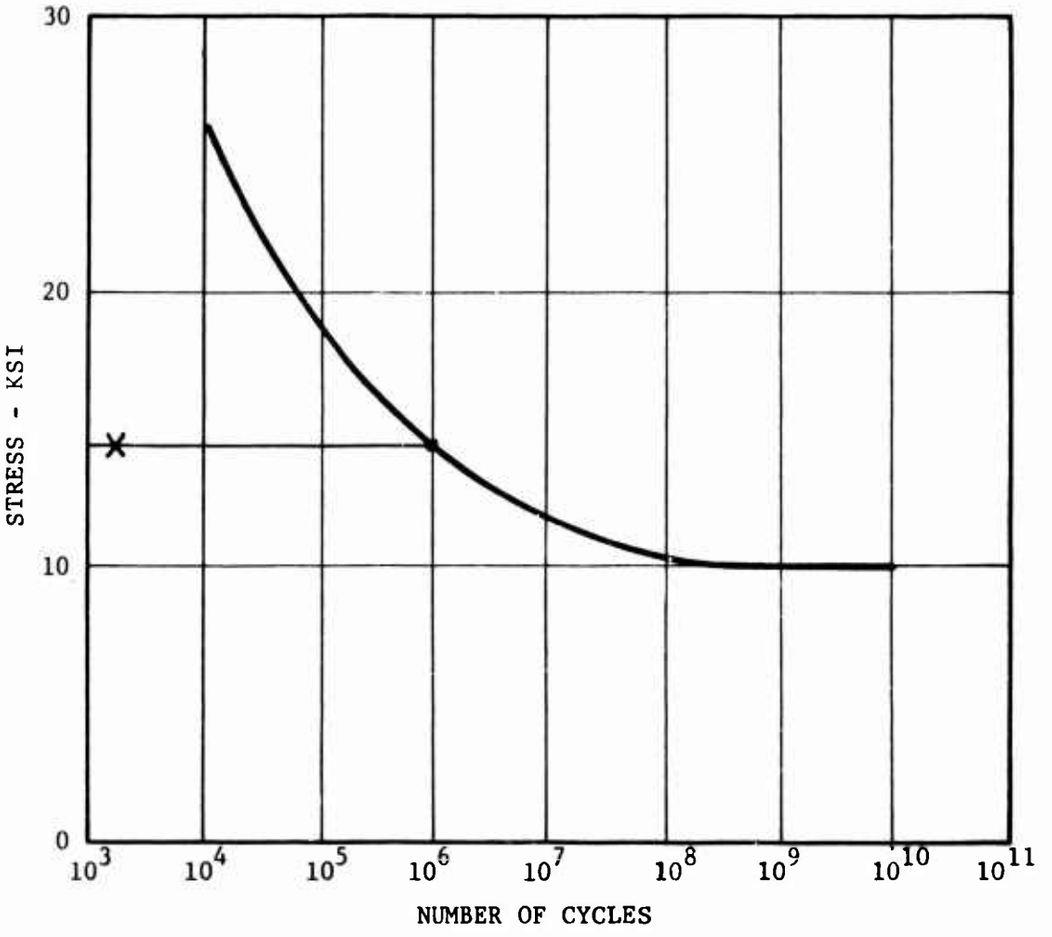

Figure 20. Typical S/N Curve for Material Used.

CONCLUSIONS AND RECOMMENDATIONS

The results of the design and test phases conducted in this program clearly show that the inductive sensing system has undergone a significant step in its ability to detect early fatigue damage. The rotating probe concept developed and applied in this work is a significant advancement in the state of the art in nondestructive testing. A comparison of the results shown in the tables herein with the results presented in the final report on the previous contract (USAAVLABS Technical Report 69-97) shows a significant improvement in the ability of the system to detect fatigue damage under identical conditions, and the microanalytic techniques employed previously guarantee the validity of the present data. The rotating probe concept as applied in this work demonstrates the eminent feasibility of this approach to a crack detection system.

We would recommend the following effort toward full utilization of the results of this contract:

1. Smaller probes capable of being used in close quarters must be constructed in order to realize the full capability of this advancement in the state of the art.

2. The probe and electronics system should be packaged for field use, and evaluated under field conditions.

3. The hypothesis relating to low cycle fatigue discussed in the preceding section should be carefully examined and verified experimentally in order to approach the question of remaining life of a structure.